

## Motion Planning for a Three-Limbed Climbing Robot in Vertical Natural Terrain

Timothy Bretl and Stephen Rock

Aerospace Robotics Lab  
Department of Aeronautics and Astronautics  
Stanford University, Stanford, CA 94305  
{tbretl, rock}@sun-valley.stanford.edu

Jean-Claude Latombe

Robotics Laboratory  
Computer Science Department  
Stanford University, Stanford, CA 94305  
latombe@cs.stanford.edu

### Abstract

*This paper presents a general framework for planning the quasi-static motion of a three-limbed climbing robot in vertical natural terrain. The problem is to generate a sequence of, continuous one-step motions between consecutive holds that will allow the robot to reach a particular goal hold. A detailed algorithm is presented to compute a one-step motion considering the equilibrium constraint only. The overall framework combines this local planner with a heuristic search technique to generate a complete plan. An online implementation of the algorithm is demonstrated in simulation.*

### 1 Introduction

The work presented in this paper is part of an effort to develop critical technologies that will enable the design and implementation of an autonomous robot able to climb vertical natural terrain. To our knowledge, this capability has not been demonstrated previously for robotic systems. Prior approaches have dealt with artificial terrain, either using special "grasps" (e.g., pegs, magnets) adapted to the terrain's surface or exploiting specific properties or features of the terrain (e.g., ducts and pipes) [1-12].

Developing this capability will further our understanding of how humans perform such complex tasks as climbing and scrambling in rugged terrain. This may prove useful in the future development of sophisticated robotic systems that will either aid or replace humans in the performance of aggressive tasks in difficult terrain. Examples include robotic systems for such military and civilian uses as search-and-rescue, reconnaissance, and planetary exploration.

Many issues need to be addressed before real robots can climb real, vertical natural terrain. This paper presents preliminary work in the area of motion planning. A general framework for climbing robots is presented and this framework is instantiated to compute climbing motions of the three-limbed robot shown in Figure 1.

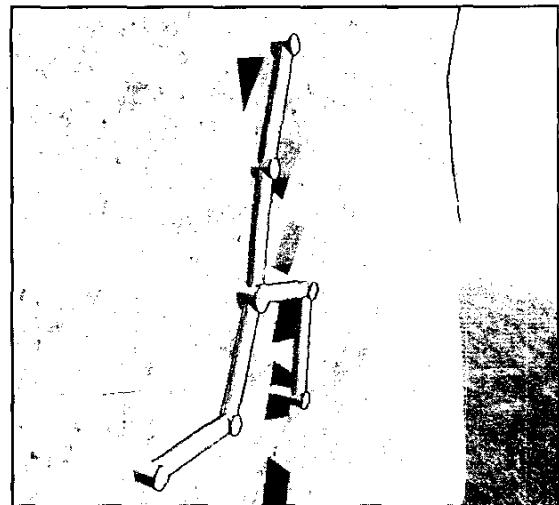


Fig 1. A three-limbed climbing robot moving vertically on natural surfaces.

#### 1.1 Problem Statement

The robot of Figure 1 consists of three limbs. Each limb has two joints, one located at the center of the robot (called the pelvis) and one at the midpoint of the limb. Motion is assumed to be quasi-static (as is usually the case in human climbing) and to occur in a vertical plane, with gravity. The low complexity of this robot's kinematics makes it suitable for studying the planning of climbing motions.

The terrain is modeled as a vertical plane to which is attached a collection of small, angled, flat surfaces, called "holds," that are arbitrarily distributed. The endpoint of each robot limb can push or pull at a single point on each hold, exploiting friction to avoid sliding.

A climbing motion of the robot consists of successive steps. Between any two consecutive steps, all three limb endpoints achieve contact with distinct holds. During each step, one limb moves from one hold to another, while the other two endpoints remain fixed. The robot can use the degrees of freedom in the linkage formed by the corre-

sponding two limbs to maintain quasi-static equilibrium and to avoid sliding on either of the two supporting holds. In addition, during a step, the torque at any joint should not exceed the actuator limits and the limbs should not collide with one another. These constraints define the feasible subset of the configuration space of the robot in each step. A path in this subset defines a one-step motion.

The overall planning problem is the following: given a model of the terrain, an initial robot configuration where it rests on a pair of holds, and a goal hold, generate a series of one-step motions that will allow the robot to move in quasi-static equilibrium from the initial configuration to an end configuration where one limb endpoint is in contact with the goal hold.

This paper presents an algorithm to compute a one-step motion considering the equilibrium constraint only. Adding the actuator-limit and self-collision constraints, though still undone, does not seem to raise major difficulties. The overall planner combines this "local planner" with a heuristic search technique to determine a sequence of holds from the initial configuration to the goal hold.

## 1.2 Related Work

The search space, which will be described in Section 3, is a hybrid space, involving both continuous and discrete actions. Many different methods are available for motion planning through continuous spaces, including cell decomposition, potential field, and roadmap algorithms [13]. Discrete actions can be included in these methods directly, such as at the level of node expansion in a roadmap algorithm, but this approach generally leads to a slow implementation that is specific to a particular system.

Previous work on motion planning for legged robots has developed tools for addressing these hybrid search spaces for some systems. This work can be categorized by whether or not the planning is done offline, in order to generate a reactive gait, or online, in order to allow non-gaited motion specific to a sensed environment.

Gaited planners generate a predefined walking pattern offline, assuming a regular environment. This pattern is used with a set of heuristics or behaviors to control the robot online based on current sensor input. Gaited planning was used by [2, 11], for example, to design patterns for climbing pipes and ducts. Other methods such as [14] are based on the notion of support triangles for maintaining equilibrium. Stability criteria such as the zero-moment-point have been used to design optimal walking gaits [15]. Dynamic gaiting and bounding also have been demonstrated [16-18]. Recent work [19, 20] has attempted to provide unifying mathematical tools for gait generation. Each of these planning algorithms would be very effective in portions of a natural climbing environment with a sustained feature such as a long

vertical crack of nearly uniform width. However, something more is needed for irregular environments such as the one studied in this paper, where the surfaces on which the robot climbs are angled and placed arbitrarily.

Non-gaited planners use sensed information about the environment to create feasible motion plans online. Most previous work on non-gaited motion planning for legged robots has focused on a particular system model, the spider robot. The limbs of a spider robot are assumed to be massless, which leads to elegant representations of their free space for quasi-static motion based on support triangles [21-23]. These methods have been extended to planning dynamic motions over rough terrain [24, 25]. The analysis used in these methods breaks down, however, when considering robots that do not satisfy the spider-robot assumption. For example, additional techniques were necessary in [26, 27] to plan non-gaited walking motions for humanoids, which clearly do not satisfy this assumption. To address the high number of degrees of freedom and the high branching factor of the discrete search through possible footsteps, these techniques were based on heuristic discretization and search algorithms. This paper considers a robot with fewer degrees of freedom in a more structured search space where it is possible to achieve much better performance than with these heuristic methods. Similar issues were addressed by [28] in designing a motion-planning algorithm for character animation, although this algorithm was meant to create "realistic," rather than strictly feasible, motion.

There is also some similarity between non-gaited motion planning for legged locomotion and for grasping and robotic manipulation, particularly in the concept of a manipulation graph [29-32]. Both types of planning require making discrete and continuous choices.

## 1.3 Contribution

The major contribution of this paper is a detailed analysis of one-step motion for the three-limbed climbing robot.

First, the properties of the continuous configurations at which the robot is in equilibrium are established. These properties are used to define the feasible set of robot configurations at each pair of holds. In particular, it is shown that the connectivity of the four-dimensional continuous feasible space of the robot can be preserved when planning in a two-dimensional subspace. This result reduces the complexity of the one-step planning problem and leads to a fast, online implementation.

Then, an overall framework is presented for planning a sequence of one-step motions from a specific configuration on an initial pair of holds to a goal hold. Heuristic methods are used to guide this discrete search, based on observation of the way in which human climbers plan their motions.

## 2 Notation and Terminology

Figure 2 illustrates the notation and terms used in the rest of this paper to describe the three-limbed robot.

The robot consists of three identical limbs meeting at the *pelvis*, whose location is denoted by  $(x_C, y_C)$ . Each limb consists of two segments and has two revolute joints, one located at the pelvis, the other between the two segments. For simplicity, the six limb segments are assumed to have equal mass and length  $L$ , but this assumption can be relaxed easily. In total, the robot's configuration space has six dimensions (two for each limb). It is assumed that the revolute joints are not limited by any internal mechanical stops.

In Figure 2, the endpoints of the two limbs of the robot are at *holds* 1 and 2 located at  $(x_1, y_1)$  and  $(x_2, y_2)$ , while the third limb is moving. The two-limbed linkage between  $(x_1, y_1)$  and  $(x_2, y_2)$  is called the *contact chain* and the other limb is the *free limb*. The constraint that two limb endpoints be at  $(x_1, y_1)$  and  $(x_2, y_2)$  reduces the set of possible configurations of the robot to a four-dimensional subspace, which is denoted by  $C(i, j)$ , since both the contact chain and the free limb now have two degrees of freedom. Any motion of the robot maintaining these two contacts will occur in  $C(i, j)$ . The configuration of the robot in  $C(i, j)$  can be uniquely specified by the angles  $(\theta_1, \theta_2)$  of the free limb, the position  $(x_C, y_C)$  of the pelvis, and two additional binary variables identifying the direction of the knee bends in the contact chain (see Figure 6(a)).

The location of the robot's center of mass (CM), which is not shown, is  $(x_{CM}, y_{CM})$ . The location of the CM's of the contact chain and the free limb are  $(x_{CM, chain}, y_{CM, chain})$  and  $(x_{CM, free}, y_{CM, free})$ , respectively.

Friction at each hold is modeled using Coulomb's law. More precisely, each hold  $(x_1, y_1)$  and  $(x_2, y_2)$  exerts a reaction force on the corresponding limb endpoint. According to Coulomb's law, this force must point into a *friction cone* to avoid slipping (see Figure 3). The orientation  $\phi_1$  and  $\phi_2$  of each cone is normal to each hold, and the half-angle  $\Delta\phi_1$  and  $\Delta\phi_2$  of each cone is determined by each hold's coefficient of friction. For the robot to be in quasi-static equilibrium, two forces, one in each cone, must exist that exactly compensate for the gravitational force (see Section 3.1). This condition will select a subset of  $C(i, j)$ , which in this paper is called the *feasible space* and is denoted by  $F(i, j)$ . Any motion of the robot maintaining both contact at the two holds and quasi-static equilibrium must occur in  $F(i, j)$ .

Since the three limbs are identical, there is no need to identify them. In particular, the same configurations can be achieved by the robot while maintaining contact at two holds, independent of which two limbs form the contact chain. It is also assumed that the robot does not bring two limb endpoints to the same hold.

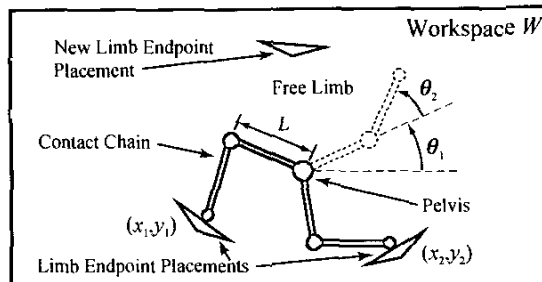


Fig. 2. The different components of the three-limbed climbing robot.

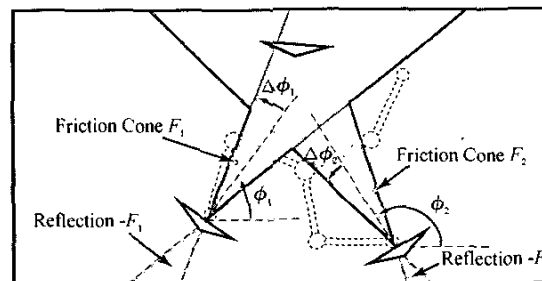


Fig. 3. The friction cones for two limb endpoint placements.

## 3 Equilibrium Analysis

In this section, it is assumed that the robot rests on two given holds  $i$  and  $j$ , as in Figures 2 and 3. This section establishes properties of the configurations in  $C(i, j)$  at which the robot is in equilibrium. These properties define the feasible subspace  $F(i, j)$ .

### 3.1 Equilibrium Constraint

The only external forces acting on the robot are gravity and the reaction forces at the two holds. The gravitational force acts at the robot's center of mass, the position of which varies as the robot moves. The two reaction forces act at the endpoints of the contact chain, which have fixed positions. Therefore, the equilibrium constraint can be represented completely by a condition on the location of the center of mass.

The work in [33, 34] provides criteria for static equilibrium in a two-dimensional workspace. In particular, it notes that if a body acted upon by gravity and two external forces is in equilibrium, it will remain so with arbitrary vertical translation of its center of mass. This observation yields the following proposition when the external forces are subject to friction constraints:

*Proposition 1.* Consider an articulated body that is acted upon by a gravitational force  $-g\hat{y}$  at  $(x_{CM}, y_{CM})$  and that is in contact with two surfaces at points  $(x_1, y_1)$  and  $(x_2, y_2)$  with associated friction cones  $F_1$  and  $F_2$ . Contact forces

can be chosen to place the body in static equilibrium without slipping if and only if there exists  $y \in \mathbf{R}$  and unit vectors  $\hat{f}_1 \in F_1$ ,  $\hat{f}_2 \in F_2$  such that the following conditions hold:

- (1a)  $(\hat{f}_1 + \hat{f}_2) \cdot \hat{y} > 0$
- (1b)  $(\hat{f}_1 \cdot \hat{x})(\hat{f}_2 \cdot \hat{x}) \leq 0$
- (1c) Lines through  $(x_1, y_1)$  and  $(x_2, y_2)$  parallel to  $\hat{f}_1$  and  $\hat{f}_2$ , respectively, intersect at  $(x_{CM}, y)$ .

This proposition allows the equilibrium of the robot to be tested given the location of its center of mass. For example, Figure 4(a) shows a configuration of the climbing robot and illustrates graphically that all three conditions in the proposition are verified, so the robot is in equilibrium. However, the proposition does not specify the shape of the equilibrium region—the region in which the center of mass must lie—although it does indicate that this region must be a union of vertical columns in the workspace.

In fact, using Proposition 1 it can be shown that the equilibrium region is always a *single* vertical column, whose boundaries are easy to calculate. This result, stated as Proposition 2, can be explained intuitively. In two dimensions, the center of mass of a body resting at two points on horizontal supporting surfaces can only vary between these two points. Rotating the support surfaces can only lead to widening or narrowing the vertical column. However, the formal proof given below is more technical.

**Proposition 2.** Consider the articulated body of Proposition 1. The region over which  $(x_{CM}, y_{CM})$  can vary while this body remains in static equilibrium is a single vertical column in the workspace.

*Proof.* From Proposition 1, it is clear that the equilibrium region is defined by the projection on the  $x$ -axis of the set of all points  $(x, y)$  for which unit vectors  $\hat{f}_1 \in F_1$ ,  $\hat{f}_2 \in F_2$  can be found satisfying Conditions 1a-1c. The problem is that this set of points is not convex, and in fact is not necessarily connected. However, it can be broken down into the union of convex sets, each of which projects to a connected segment on the  $x$ -axis. Further, it can be shown that each projected segment overlaps in such a way that the entire  $x$ -projection is a single connected segment, proving the result.

Assume without loss of generality that  $x_2 > x_1$ , that  $x_1 \neq x_2$  ( $x_1 = x_2$  is a degenerate case that can be handled separately), and that each friction cone has a half-angle  $\Delta\phi < 90^\circ$  (true for flat contact surfaces).

First, notice that a point  $(x, y)$  satisfies Condition 1c only if it lies in the intersection  $(F_1 \cup -F_1) \cap (F_2 \cup -F_2)$ . Call the set of points that additionally satisfy Conditions 1a-1b the set of *feasible* intersection points for cones  $F_1$  and  $F_2$ . The equilibrium region is the  $x$ -projection of this set.

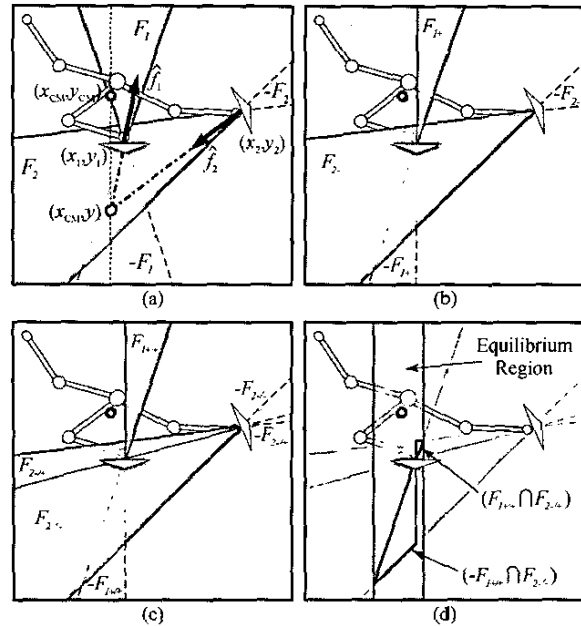


Fig. 4. An example calculation of the equilibrium region associated with a set of limb endpoint placements for the three-limbed robot.

Next, divide each friction cone  $F_1$  and  $F_2$  into two parts. Let  $F_{1+}$  be that part of  $F_1$  containing points such that  $x > x_1$ , and  $F_{1-}$  be that part of  $F_1$  containing points such that  $x < x_1$ . Likewise, divide  $F_2$  into  $F_{2+}$  and  $F_{2-}$  using  $x_2$ . Since each friction cone has a half-angle  $\Delta\phi < 90^\circ$ , each of  $F_{1+}$ ,  $F_{1-}$ ,  $F_{2+}$ , and  $F_{2-}$  must be either a single cone or empty.

Since Condition 1b indicates that force vectors must lie in opposite  $x$ -directions, the set of feasible intersection points for the cones  $F_1$  and  $F_2$  is equal to the union of the set of feasible intersection points for  $F_{1+}$  and  $F_{2-}$ , facing inward, and  $F_{1-}$  and  $F_{2+}$ , facing outward. For example, since  $F_{2+}$  is empty for the two friction cones shown in Figure 4(a), only the intersection of the inward-facing cones  $F_{1+}$  and  $F_{2-}$  needs to be considered, as shown in Figure 4(b).

For inward-facing cones, condition 1a can be used to show that the set of feasible intersection points  $(x, y)$  must satisfy  $(y - y_1)(x - x_2) > (y - y_2)(x - x_1)$ . Further divide  $F_{1+}$  into the cones  $F_{1++}$ , containing points such that  $(y - y_1)(x_2 - x_1) > (y_2 - y_1)(x - x_1)$ , and  $F_{1+-}$ , containing points such that  $(y - y_1)(x_2 - x_1) < (y_2 - y_1)(x - x_1)$ . Analogously, divide  $F_{2-}$ . This procedure, shown in Figure 4(c), simply divides the friction cones into the part that points above the line connecting  $(x_1, y_1)$  and  $(x_2, y_2)$  and the part that points below this line. Again, since each friction cone has a half-angle  $\Delta\phi < 90^\circ$ , each of the sub-cones must be either a single cone or empty.

Then from condition 1a, the set of feasible intersection points for the inward-facing cones is exactly the union of subsets  $(-F_{1++} \cap F_{2--}) \cup (F_{1+-} \cap F_{2--}) \cup (F_{1+-} \cap -F_{2--})$ , as shown in Figure 4(d).

Each of these three subsets is the intersection of two convex cones, so is convex with an  $x$ -projection that is a

single connected segment. Further, it is easy to show that if any two subsets are nonempty, their  $x$ -projections must overlap at either  $x_1$  or  $x_2$ , as is the case in Figure 4(d). Therefore, the  $x$ -projection of the set of feasible intersection points for inward-facing cones is a single connected segment.

An identical argument shows the same result for the set of outward-facing cones. In addition, it is easy to show that if the  $x$ -projections for both the inward- and outward-facing cones are nonempty, then they must overlap at either  $x_1$  or  $x_2$ . Thus, the  $x$ -projection for the entire set of feasible intersection points is a single connected segment, proving Proposition 2.  $\square$

### 3.2 Feasible Space for a Given Pelvis Location

Given knee bend directions as described in Section 2, the configuration of the three-limbed climbing robot is uniquely specified by the position  $(x_C, y_C)$  of the pelvis and the angles  $(\theta_1, \theta_2)$  of the free limb. This section first establishes an analytical expression of the feasible space  $\Theta_{FL}$  of the free limb given  $(x_C, y_C)$ . Next, this expression is used to characterize the connectivity of  $\Theta_{FL}$  in Proposition 3.

Since the location of the CM of the contact chain is fixed by the given  $(x_C, y_C)$ , the equilibrium region shown in Section 3.1 to be a vertical column defined by some  $(x_{min}, x_{max})$  can be transformed from a constraint on the location of the CM of the entire robot to a constraint on the CM of the free limb only. Under the geometry and mass assumptions made in Section 2, the following relationship holds:

$$x_{CM, free} = (3x_{CM} - 2x_{CM, chain}) \quad (1)$$

So, the center of mass of the free limb must be within the column  $(x_{min, free}, x_{max, free})$  in the workspace where

$$x_{min, free} = (3x_{min} - 2x_{CM, chain}) \quad (2)$$

$$x_{max, free} = (3x_{max} - 2x_{CM, chain})$$

A pelvis location  $(x_C, y_C)$  is feasible with respect to the equilibrium constraint only if a configuration of the free limb exists such that  $x_{CM, free} \in [x_{min, free}, x_{max, free}]$ . The center of mass of the free limb is located at

$$x_{CM, free} = x_C + \frac{1}{4}(3\cos\theta_1 + \cos(\theta_1 + \theta_2)) \quad (3)$$

From Equations (1)-(3), a pelvis location is feasible only if

$$\begin{aligned} x_{min, free} &\geq x_C - L \\ x_{max, free} &\leq x_C + L \end{aligned} \quad (4)$$

$$x_{min, free} \leq x_{max, free}$$

For any feasible pelvis location, the equilibrium region of the center of mass of the free limb can be cropped such that  $[x_{min, free}, x_{max, free}] \subset [x_C - L, x_C + L]$ , since values outside these bounds are unattainable.

The solutions of Equation 3 for a fixed value of  $x_{CM, free}$  define a one-dimensional curve in the configuration space of the free limb. Curves for several values of  $x_{CM, free}$  are

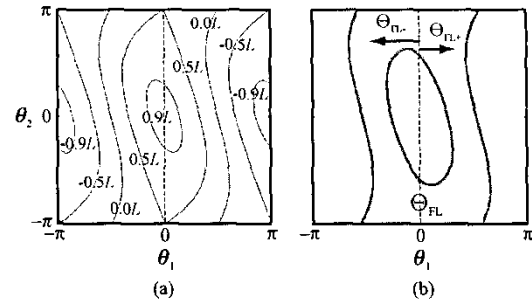


Fig. 5. Calculating the feasible space  $\Theta_{FL}$  of the free limb for a given pelvis location.

shown in Figure 5(a). Since the mapping from  $(\theta_1, \theta_2)$  to  $x_{CM, free}$  is single-valued, no two such curves intersect. The feasible space  $\Theta_{FL}$  of the free limb is the region between the solution curves for  $x_{CM, free} = x_{min, free}$  and  $x_{CM, free} = x_{max, free}$  as shown in Figure 5(b) for  $(x_{min, free}, x_{max, free}) = (x_C - 0.1L, x_C + 0.7L)$ .

Since the feasible space  $\Theta_{FL}$  depends on both  $x_C$  and  $x_{CM, chain}$ , which itself is a complicated function of  $(x_C, y_C)$ , it is difficult to compute the four-dimensional feasible space of the robot. However, the following proposition characterizes the connectivity of this space:

**Proposition 3.** Partition  $\Theta_{FL}$  as

$$\begin{aligned} \Theta_{FL-} &= \Theta_{FL} \cap \{(\theta_1, \theta_2) | \theta_1 \leq 0\} \\ \Theta_{FL+} &= \Theta_{FL} \cap \{(\theta_1, \theta_2) | \theta_1 \geq 0\} \end{aligned} \quad (5)$$

Also, for any  $x' \in [x_C - L, x_C + L]$ , define

$$\begin{aligned} (\theta_1, \theta_2)_{x'-} &= (-\cos^{-1} \frac{x' - x_C}{L}, 0) \\ (\theta_1, \theta_2)_{x'+} &= (\cos^{-1} \frac{x' - x_C}{L}, 0) \end{aligned} \quad (6)$$

Then the following results hold:

- (3a) Let  $\tilde{x} \in [x_{min, free}, x_{max, free}]$ . Then  $(\theta_1, \theta_2)_{\tilde{x}+} \in \Theta_{FL+}$  and  $(\theta_1, \theta_2)_{\tilde{x}-} \in \Theta_{FL-}$ .
- (3b)  $\Theta_{FL+}$  and  $\Theta_{FL-}$  are both connected spaces.
- (3c)  $\Theta_{FL}$  is connected if and only if
 
$$\begin{aligned} x_{min, free} &\notin [x_C - \frac{L}{2}, x_C + \frac{L}{2}] \text{ or} \\ x_{max, free} &\notin [x_C - \frac{L}{2}, x_C + \frac{L}{2}]. \end{aligned}$$

*Proof.* Result 3a follows trivially, since  $(\theta_1, \theta_2)_{x'-}$  and  $(\theta_1, \theta_2)_{x'+}$  are solutions to Equation 3 for  $x_{CM, free} = \tilde{x}$  such that  $\theta_1 \leq 0$  and  $\theta_1 \geq 0$ , respectively. This result implies that any attainable value of  $x_{CM, free}$  is attainable with  $\theta_2 = 0$ , and that continuous paths between two values of  $x_{CM, free}$  for  $\theta_2 = 0$  always exist in both  $\Theta_{FL-}$  and  $\Theta_{FL+}$ . Since the boundary of  $\Theta_{FL+}$  is defined by curves of constant  $x_{CM, free}$ , and since, as mentioned above, these curves do not intersect, then a curve of constant  $x_{CM, free} = \tilde{x}$  between  $(\theta_1, \theta_2) \in \Theta_{FL+}$  and  $(\theta_1, \theta_2)_{\tilde{x}+}$  that lies completely within  $\Theta_{FL+}$  always exists. So a path between any two configurations  $(\theta_1, \theta_2)_i \in \Theta_{FL+}$  and  $(\theta_1, \theta_2)_f \in \Theta_{FL+}$  can always be generated by moving from  $(\theta_1, \theta_2)_i$  along a curve of constant  $x_{CM, free} = \tilde{x}_i$  to  $(\theta_1, \theta_2)_{\tilde{x}+}$ , moving along  $\theta_2 = 0$  to  $(\theta_1, \theta_2)_{\tilde{x}f+}$ , and moving along a curve of constant

$x_{CM,free} = \tilde{x}_f$  to  $(\theta_1, \theta_2)$ . Therefore,  $\Theta_{FL+}$  is connected. The result for  $\Theta_{FL-}$  follows identically, so Result 3b holds. To prove Result 3c, notice that  $\Theta_{FL}$  is connected if and only if some  $(\theta_1, \theta_2) \in \Theta_{FL}$  exists such that  $\theta_1=0$  or  $\theta_1=\pm\pi$ . From Equation 3, this is equivalent to saying that  $x_{CM,free} \notin [x_C - \frac{\ell}{2}, x_C + \frac{\ell}{2}]$  at some  $(\theta_1, \theta_2) \in \Theta_{FL}$ , which from Result 3b can occur if and only if either  $x_{min,free} \notin [x_C - \frac{\ell}{2}, x_C + \frac{\ell}{2}]$  or  $x_{max,free} \notin [x_C - \frac{\ell}{2}, x_C + \frac{\ell}{2}]$ .  $\square$

### 3.3 Implications

Proposition 3 implies that for any feasible pelvis location the feasible space of the free limb can be divided into two non-empty, connected components,  $\Theta_{FL+}$  and  $\Theta_{FL-}$ . Therefore, using Result 3a it is possible to extend any feasible continuous path of the pelvis to a feasible path of the entire robot, such that the configuration of the free limb remains in either  $\Theta_{FL+}$  or  $\Theta_{FL-}$ . This key result yields the continuous planning approach described in this section to compute one-step motions of the robot.

First, decompose the four-dimensional feasible space  $F(i,j)$  into four subsets as illustrated in Figure 6(a). Each subset corresponds to a pair of knee bends in the limbs forming the contact chain. In each subset, the position of the CM of the contact chain is uniquely determined by the position of the pelvis. Therefore, the feasibility of a pelvis location in each subset is determined by Equation 4. Transitions between subsets can occur only within one-dimensional curves along their boundaries, which correspond to feasible positions of the pelvis in which one of the limbs is fully stretched out.

Further partition each subset into two parts according to the sign of the configuration parameter  $\theta_1$  of the free limb, as illustrated in Figure 6(b). In one subset ( $\theta_1 \geq 0$ ), the first segment of the free limb points upward; in the other subset, it points downward. Notice that the sign of  $\theta_1$  also serves to distinguish  $\Theta_{FL+}$  from  $\Theta_{FL-}$ , so robot configurations in each of the two parts of each subset correspond to free limb configurations entirely in either  $\Theta_{FL+}$  or  $\Theta_{FL-}$ . Transitions between the two parts can occur only within two-dimensional regions where  $\Theta_{FL}$  is connected, i.e. where the conditions of Result 3c are satisfied.

Suppose for a pair of holds  $(i,j)$  that in each of the four subsets shown in Figure 6(a) an explicit representation can be built of the two-dimensional region formed by the feasible positions of the pelvis. From Proposition 3, this region is identical in the two parts of each subset corresponding to  $\Theta_{FL+}$  and  $\Theta_{FL-}$ . Therefore, the connected components of each of the eight subsets shown in Figure 6(b) can be determined. Likewise, suppose that an explicit representation can be built of the one-dimensional transition curves between the subsets corresponding to different knee bends and of the two-dimensional transition regions between the parts of each of these subsets corresponding to  $\Theta_{FL+}$  and  $\Theta_{FL-}$ . Using these transition

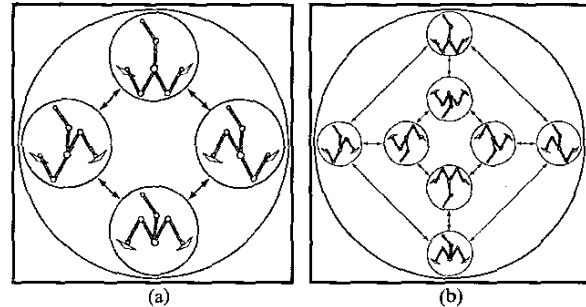


Fig. 6. Decompositions of  $F_P(i,j)$  into four sub-spaces based on knee bends and into eight sub-spaces based additionally on whether the free limb is pointing up or down.

curves and regions, the connected components of each of the eight subsets can be linked to form a discrete graph.

Components of this graph are the connected components of the two-dimensional space of feasible pelvis positions of the robot. This space, which is denoted  $F_P(i,j)$ , is the projection of  $F(i,j)$  onto  $(x_C, y_C)$ . To plan a continuous path between any two points in a connected component of  $F(i,j)$ , it suffices to plan a path in the corresponding component of  $F_P(i,j)$ . This path can then be lifted to  $F(i,j)$  using Proposition 3. Define a distinct state for each such connected component of  $F_P(i,j)$ , and denote it  $(i,j)_A$ ,  $(i,j)_B$ , etc.

Finding analytic representations of  $F_P(i,j)$  and the transition regions is impractical. In the current implementation, these regions are constructed using probabilistic roadmaps similar to those in [35]. For the three-limbed robot, a deterministic two-dimensional grid approximation would work as well. However, this approach might scale poorly to climbing robots with more than three limbs.

## 4 Overall Planning Framework

This section describes an overall framework for planning a sequence of one-step motions from a specific configuration on an initial pair of holds to a goal hold.

### 4.1 Search Space

The search space for the three-limbed climbing robot is a hybrid space, involving both continuous and discrete actions. Discrete actions correspond to placing a limb endpoint on a hold or removing it from the hold. They decompose the overall climbing motion into a sequence of steps. During each step, two limb endpoints are positioned at two given holds and the action is a continuous motion that brings the endpoint of the free limb from one hold to another. Therefore, motion planning can be divided into *discrete planning* and *continuous planning* operations, each with its own search space.

Section 3 described the continuous-planning search space of the robot, when its limbs are in contact with two

holds  $i$  and  $j$ , and presented a method of generating the components of the feasible part of this space (e.g.  $(i,j)_A$ ,  $(i,j)_B$ , etc.).

The discrete-planning search space is the collection of all of these components, for all pairs of holds  $(i,j)$  in the workspace. So, each state in this search space is a single component  $(i,j)_M$  of  $F_P(i,j)$ . Each possible successor of a state  $(i,j)_M$  is another state of the form  $(i,k)_N$  or  $(j,k)_O$ , which is a single component of  $F_P(i,k)$  or  $F_P(j,k)$  for a different pair of holds  $(i,k)$  or  $(j,k)$ .

A link to a successor is a robot configuration with limbs in contact with holds  $i$ ,  $j$ , and  $k$ , that satisfies two conditions. First, the position of the pelvis in this configuration must be common to both  $(i,j)_M$  and  $(i,k)_N$  (or  $(j,k)_O$ ). Second, the four-dimensional representation of this configuration in  $C(i,j)$  and  $C(i,k)$  (or  $C(j,k)$ ) must be in  $F(i,j)$  and  $F(i,k)$  (or  $F(j,k)$ ), respectively. The second condition must be satisfied because the link defines a *specific* free-limb configuration, while the components  $(i,j)_M$  and  $(i,k)_N$  (or  $(j,k)_O$ ) specify *compliant* free-limb configurations only. Note that this is the only point in the planning process at which  $F(i,j)$ , rather than  $F_P(i,j)$ , need be considered. In the current implementation, these link configurations are generated using a random sampling technique.

For example, consider the environment shown in Figure 7(a). The robot is initially located on holds  $(0,1)$  with a goal of reaching hold 4. The discrete-planning search space is shown in Figure 7(b). In this example, only  $F_P(2,3)$  has more than one component,  $(2,3)_A$  and  $(2,3)_B$ .

## 4.2 Algorithm

In practice, it is too costly to compute the entire search space online for a reasonably sized environment. Instead, heuristic methods are used to guide the discrete search and the components of  $F_P(i,j)$  are only computed as each pair of holds  $(i,j)$  is explored.

For example, a necessary condition for a link between two pairs of holds  $(i,j)$  and  $(i,k)$  is that holds  $i$  and  $k$  be distant by less than  $2L$ . Likewise, the equilibrium regions  $(x_{min}, x_{max})$  for both pairs of holds (see Section 3.1) must overlap. These simple conditions make it possible to quickly filter out many successor holds.

Another useful heuristic is to pre-compute rough discrete plans, without any continuous-planning exploration, using conservative approximations for the components  $(i,j)_M$  of each  $F_P(i,j)$ . In almost all cases, it has been found that each of the eight subsets illustrated in Figure 6(b) contains a *single* connected component. Using this decomposition, the entire discrete search space can be computed online. The resulting nominal plan is then used to guide a discrete search using the exact decomposition of every  $F_P(i,j)$ .

The appropriateness of this approach is motivated by observation of the way in which human climbers plan

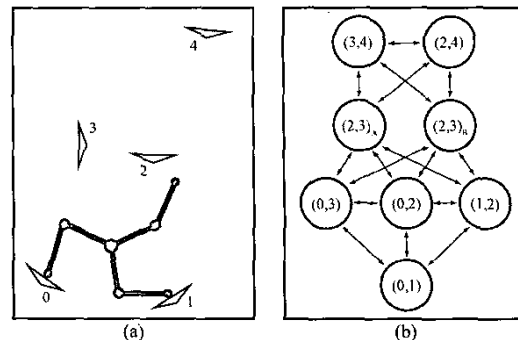


Fig. 7. An example environment for the three-limbed climbing robot and the corresponding connectivity graph between discrete states.

their motion. The resulting path, often called a *sequence*, consists of a series of *moves*, such as a back-step or high-step, between an ordered set of hand and foot placements (see [36, 37]). Each move does not specify a continuous path, but rather a discrete choice that is exactly analogous to the selection of knee-bend directions for the three-limbed robot.

Future observation of human climbers may suggest other useful heuristics, such as a consideration of the size of equilibrium regions.

## 5 Simulation

Figure 8 shows the result of applying the planning algorithm described in Sections 3 and 4 to move the three-limbed robot through the simulated vertical terrain illustrated in Figure 7(a). Notice that the center of mass of the robot stays within the equilibrium region, as required.

Other results, including animations of 3D-simulations, are available online at <http://arl.stanford.edu/~tbrettl/>.

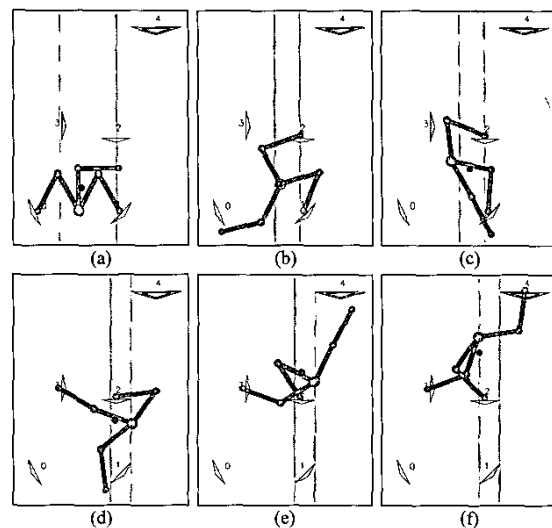


Fig. 8. Results of a simulation, shown as a time-sequence.

## 6 Future Work

This paper presented a framework for planning the motion of a three-limbed climbing robot in vertical terrain and showed the results of applying this framework in simulation. Current work concerns the application of the planning algorithm to experimental hardware. As part of this effort, the continuous-planning method described in Section 3 is being extended to handle additional motion constraints, more complicated robot geometries, imperfectly known environments, and three-dimensional terrain. Future work will address other fundamental issues such as sensing, control, hardware design, and grasping.

**Acknowledgements** T. Bretl is partially supported by an NDSEG fellowship through the ASEE and by a Herbert Kunzel Fellowship. The authors would also like to thank D. Halperin and T. Miller for their helpful contributions.

## References

- [1] P. Pirjanian, C. Leger, E. Mumm, B. Kennedy, M. Garrett, H. Aghazarian, S. Farritor, and P. Schenker, "Distributed Control for a Modular, Reconfigurable Cliff Robot," *IEEE Int. Conf. on Robotics and Automation*, 2002.
- [2] A. Madhani and S. Dubowsky, "Motion Planning of Mobile Multi-Limb Robotic Systems Subject to Force and Friction Constraints," *IEEE Int. Conf. on Robotics and Automation*, 1992.
- [3] S. Hirose, K. Yoneda, and H. Tsukagoshi, "Titan VII: Quadruped Walking and Manipulating Robot on a Steep Slope," *IEEE Int. Conf. on Robotics and Automation*, 1997.
- [4] M. Nilsson, "Snake Robot - Free Climbing," in *IEEE Control Systems Magazine*, vol. 18, Feb 1998, pp. 21-26.
- [5] J. C. Grieco, M. Prieto, M. Armada, and P. G. d. Santos, "A Six-Legged Climbing Robot for High Payloads," *IEEE Int. Conf. on Control Applications*, 1998.
- [6] H. Dulimarta and R. L. Tummala, "Design and Control of Miniature Climbing Robots with Nonholonomic Constraints," 4th World Congress on Intelligent Control and Automation, Jun 2002.
- [7] S. W. Ryu, J. J. Park, S. M. Ryew, and H. R. Choi, "Self-Contained Wall-Climbing Robot with Closed Link Mechanism," *IEEE/RSJ Int. Conf. on Intelligent Robots and Systems*, 2001.
- [8] W. Yan, L. Shuliang, X. Dianguo, Z. Yanzheng, S. Hao, and G. Xueshan, "Development & Application of Wall-Climbing Robots," *IEEE Int. Conf. on Robotics and Automation*, 1999.
- [9] H. Amano, K. Osuka, and T.-J. Tam, "Development of Vertically Moving Robot with Gripping Handrails for Fire Fighting," *IEEE/RSJ Int. Conf. on Intelligent Robots and Systems*, 2001.
- [10] Z. M. Ripin, T. B. Soon, A. B. Abdullah, and Z. Samad, "Development of a Low-Cost Modular Pole Climbing Robot," *TENCON*, 2000.
- [11] W. Neubauer, "A Spider-Like Robot That Climbs Vertically in Ducts or Pipes," *IEEE/RSJ/GI Int. Conf. on Intelligent Robots and Systems*, 1994.
- [12] K. Jagnemma, A. Rzepniewski, S. Dubowsky, P. Pirjanian, T. Huntsberger, and P. Schenker, "Mobile Robot Kinematic Reconfigurability for Rough-Terrain," *Sensor Fusion and Decentralized Control in Robotic Systems III*, 2000.
- [13] J.-C. Latombe, *Robot Motion Planning*. Boston, MA: Kluwer Academic Publishers, 1991.
- [14] Y. Golubev and E. Selenskii, "The Locomotion of a Six-Legged Walking Robot in Horizontal Cylindrical Pipes with Viscous Friction," *J. of Computer and Systems Sciences Int.*, pp. 349-356, 2001.
- [15] K. i. Nagasaka, H. Inoue, and M. Inaba, "Dynamic Walking Pattern Generation for a Humanoid Robot Based on Optimal Gradient Method," *IEEE Int. Conf. on Systems, Man, and Cybernetics*, 1999.
- [16] M. Berkemeier, "Modeling the Dynamics of Quadrupedal Running," *Int. J. of Robotics Research*, vol. 17, Sep 1998.
- [17] M. Buehler, U. Saranli, D. Papadopoulos, and D. Koditschek, "Dynamic Locomotion with Four and Six-Legged Robots," *Int. Symp. on Adaptive Motion of Animals and Machines*, 2000.
- [18] M. F. Silva, J. A. T. Machado, and A. M. Lopes, "Performance Analysis of Multi-Legged Systems," *IEEE Int. Conf. on Robotics and Automation*, 2002.
- [19] B. Goodwine and J. Burdick, "Motion Planning for Kinematic Stratified Systems with Application to Quasi-Static Legged Locomotion and Finger Gaiting," 4th Int. Workshop on Algorithmic Foundations of Robotics, Mar 2000.
- [20] B. Goodwine and J. Burdick, "Controllability of Kinematic Control Systems on Stratified Configuration Spaces," *IEEE Tr. on Automatic Control*, vol. 46, pp. 358-368, 2001.
- [21] J.-D. Boissonnat, O. Devillers, and S. Lazard, "Motion Planning of Legged Robots," *SIAM J. on Computing*, vol. 30, pp. 218-246, 2001.
- [22] J.-D. Boissonnat, O. Devillers, L. Donati, and F. Preparata, "Motion Planning of Legged Robots: The Spider Robot Problem," *Int. J. of Computational Geometry and Applications*, vol. 5, pp. 3-20, 1995.
- [23] J.-D. Boissonnat, O. Devillers, and S. Lazard, "Motion Planning of Legged Robots," *Rapport de Recherche INRIA*, vol. 3214, 1997.
- [24] S. Kajita and K. Tani, "Study of Dynamic Biped Locomotion on Rugged Terrain," *IEEE Int. Conf. on Robotics and Automation*, 1991.
- [25] S. Bai, K. H. Low, and M. Y. Teo, "Path Generation of Walking Machines in 3d Terrain," *IEEE Int. Conf. on Robotics and Automation*, 2002.
- [26] J. Kuffner, Jr., S. Kagami, K. Nishiwaki, M. Inaba, and H. Inoue, "Dynamically-Stable Motion Planning for Humanoid Robots," *Autonomous Robots*, vol. 12, pp. 105-118, 2002.
- [27] J. Kuffner, Jr., K. Nishiwaki, S. Kagami, M. Inaba, and H. Inoue, "Footstep Planning among Obstacles for Biped Robots," *IEEE/RSJ Int. Conf. on Intelligent Robots and Systems*, 2001.
- [28] M. Kalisiak and M. v. d. Panne, "A Grasp-Based Motion Planning Algorithm for Character Animation," *Eurographics Workshop on Computer Animation and Simulation*, 2000.
- [29] R. Alami, J. P. Laumond, and T. Simeon, "Two Manipulation Planning Algorithms," in *Algorithmic Foundations of Robotics*, K. Goldberg, D. Halperin, J.-C. Latombe, and R. Wilson, Eds. Wellesley, MA: A K Peters, 1995, pp. 109-125.
- [30] J. Ponce, S. Sullivan, A. Sudsang, J.-D. Boissonnat, and J.-P. Merlet, "On Computing Four-Finger Equilibrium and Force-Closure Grasps of Polyhedral Objects," *Int. J. of Robotics Research*, vol. 16, pp. 11-35, Feb 1997.
- [31] A. Bicchi and V. Kumar, "Robotic Grasping and Contact: A Review," *IEEE Int. Conf. on Robotics and Automation*, 2000.
- [32] M. Yashima and H. Yamaguchi, "Dynamic Motion Planning Whole Arm Grasp Systems Based on Switching Contact Modes," *IEEE Int. Conf. on Robotics and Automation*, 2002.
- [33] R. Mason, E. Rimon, and J. Burdick, "The Stability of Heavy Objects with Multiple Contacts," *IEEE Int. Conf. on Robotics and Automation*, 1995.
- [34] R. Mason, E. Rimon, and J. Burdick, "Stable Poses of 3-Dimensional Objects," *IEEE Int. Conf. on Robotics and Automation*, 1997.
- [35] L. E. Kavraki, P. Svetska, J.-C. Latombe, and M. Overmars, "Probabilistic Roadmaps for Path Planning in High-Dimensional Configuration Spaces," *IEEE Tr. on Robotics and Automation*, vol. 12, pp. 566-580, 1996.
- [36] D. Graydon and K. Hanson, *Mountaineering: The Freedom of the Hills*, 6th Rev edition ed: Mountaineers Books, Oct 1997.
- [37] J. Long, *How to Rock Climb!*: Chockstone Press, May 2000.